Quality Evaluation of Self-Bonded SiC as Sidelining Materials in Aluminium Electrolysis Cells

Egil Skybakmoen[1], Zhaohui Wang[2], Zhigang Huang[3] and Andreas Rugaard Lund[4]
1. Research manager
2. Research scientist
SINTEF Industry, Trondheim, Norway
3. Technical director
Luoyang Institute of Refractories Research, Luoyang, China
4. International sales assistant
Simonsen, Nykøbing Mors, Denmark
Corresponding author: egil.skybakmoen@sintef.no
https://doi.org/10.71659/icsoba2025-al077

Abstract

Use of Si_3N_4-SiC is today the state of the art as sidelining materials in modern aluminium electrolysis cells. An alternative can be to use self-bonded SiC sidelining materials. A test program has been developed at SINTEF to test physical and chemical materials properties of ceramic materials. Open porosity, density, thermal expansion, thermal conductivity, oxidation resistance and chemical resistance have been measured for a self-bonded SiC material (Sicatec 95). In addition, mineral phase analysis has been performed using both XRD and LECO analysis (total O and total N) together with microstructure studies performed by SEM. In this article, the materials properties measured on self-bonded SiC will be compared to the ones of Silicon-nitride bonded SiC and industrial relevance will be discussed.

Keywords: Aluminum electrolysis cells, Sidelining materials, Self-bonded SiC

1. Introduction

With increased cell sizes and higher needs of increased productivity the performance of the cathode lining materials is more and more important and crucial for design of aluminium reduction cells. The sidelining materials today is mainly based on ceramic linings with Si_3N_4-SiC as state of the art. However, we have seen quality issues with these kind of materials due to variable microstructure and weak chemical resistance when no side ledge is present. Therefore, there is a need for an alternative material with better chemical resistance and higher thermal conductivity.

Self-bonded SiC may be an alternative material. This paper will present properties of such a material using different laboratory test methods.

2. Production of Self-Bonded SiC and Material Microstructure

Self-bonded SiC blocks are mainly produced by a mixture of SiC grains, powder (2.5–1.43 mm, 1.43–0.5 mm, 0.5–0 mm for grains, and less than 45 µm for the powder) and metal Si powder (less than 45 µm) and a binder. The binder (phenolic resin with residual carbon around 40 %) acts as a temporary bond of the green block and as the source of carbon for the formation of β-SiC. The green blocks are produced by pressing and vibrating, then dried and fired in inert (argon) atmosphere under several temperature stages up to 1400–1420 °C. N_2 gas is used for the cooling-down to protect the blocks from oxidation, and also consumes the potential residual Si to form Si_3N_4 or Si_2ON_2 (O is mainly from SiO_2 in the raw materials). The final block contains around 94–96 % of SiC and a small amount of Si_2ON_2. Fibrous β-SiC (together with Si_2ON_2) intervene and form a three-dimensional network wrapping up the SiC grains. The microstructure obtained by SEM is shown in Figure 1.

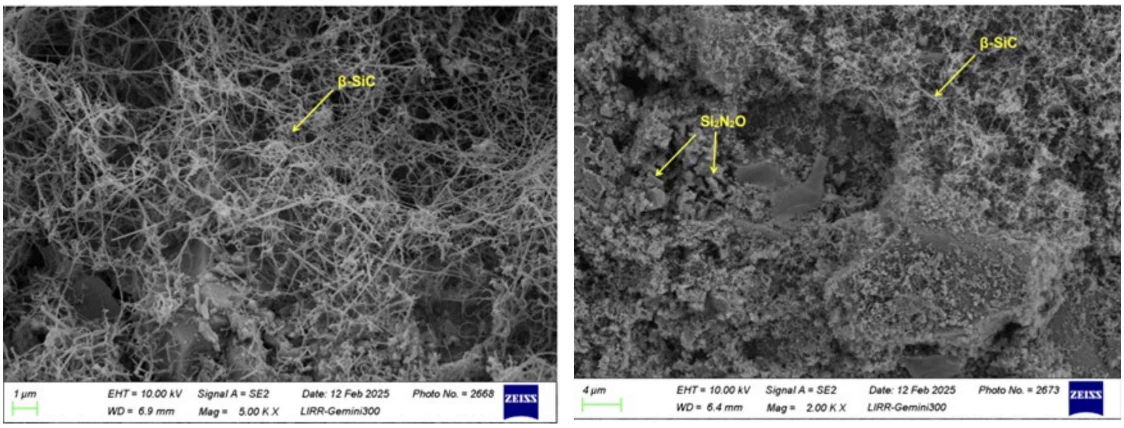

Figure 1. Microstructure of self-bonded SiC. SEM by LIRR.

XRD analysis performed by the Luoyang Institute of Refractories Research (LIRR) show contents of SiC and Si_2ON_2 as illustrated in Figure 2.

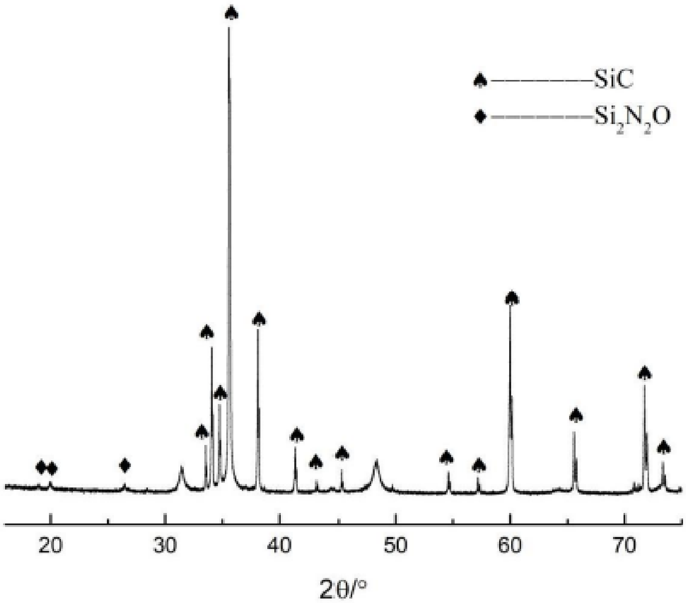

Figure 2. XRD-analysis performed by LIRR.

SINTEF performed XRD Rietveld and LECO analysis of 2 samples marked outer and inner (see Figure 3). The results are shown in Table 1.

Table 1. XRD and LECO analysis of 2 samples.

Sample	LECO (wt %)		XRD Rietveld (wt %)		
	O	N	SiC	Si_2ON_2	Si
Outer	1.52 ± 0.03	1.63 ± 0.06	93.7	6.2	0.1
Inner	1.36 ± 0.01	1.50 ± 0.03	92.6	7.3	0.1

The analysis confirmed content of mainly SiC, some Si_2ON_2 and small amount of Si.

3. Test Methods and Material Sampling

Some important properties for this material have been analysed with the test methods shown in Table 2.

Table 2. Test methods performed on self-bonded SiC samples by SINTEF.

Test parameter	Test methods	Sample size (mm)	# samples
Open porosity (%)	ISO 5017	Different	10
Density (g/cm^3)	ISO 5017	Different	10
Mineral phase analysis	XRD / LECO	Powder	2
Th. expansion, RT to 1200 °C (W/m·K)	ASTM C372	8 x 8 x 50	1
Th. conductivity, RT to 900 °C	LFA 457	12.7 diam x 2	2
Oxidation resistance, 950 °C, 100 h in air	SINTEF	60 x 30 x 15	2
Chemical resistance, 50 h	SINTEF	10 x 10 x 110	4
Chemical resistance, 24 h	LIRR	20 x 20 x 120	4

A 320 × 160 × 60 mm block weighting 8.34 kg was received. A diamond saw was used to cut the different samples needed for the tests. The full block size and the samples position for some of the tests are shown in Figure 3.

Figure 3. Full size block and sampling positions from the cut surface.

4. Test Methods and Results

4.1 Open Porosity and Density

The open porosity and density were measured for 10 samples by ISO 5017 method. The results are shown in Table 3.

Table 3. Open porosity and density for all samples.

Sample name	Open porosity (%)	Density (g/cm^3)
ChemRes-1 outer	14.17	2.72
ChemRes-2 Inner	13.66	2.74
ChemRes-3 Inner	13.48	2.74
ChemRes-4 outer	13.31	2.75
Small outer	13.57	2.74
Small inner	12.75	2.76
Oxidation outer	14.18	2.72
Oxidation inner	13.39	2.74
Th.cond outer	13.59	2.74
Th.cond inner	16.16	2.65
Average	13.83	2.73
Standard deviation	0.92	0.03

The open porosity as a function of position within the block is shown in Figure 4.

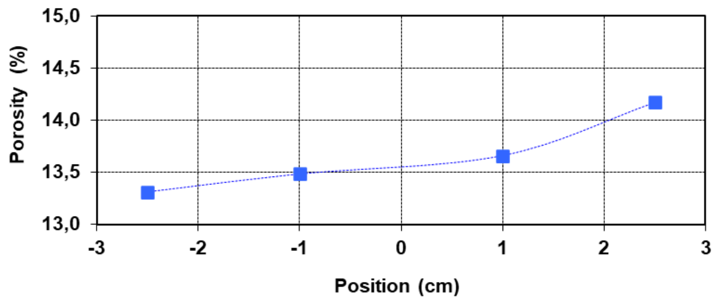

Figure 4. Open porosity as a function of position within the block, 0 is the middle of the block.

4.2 Thermal Expansion

Thermal expansion was measured according to ASTM C372 standard on a 50.0 × 8.0 ××x 8.0 mm sample. The temperature range was 20–1100 °C in an atmosphere of argon gas with a heating rate of 2 °C/min. The thermal expansion (in %) during heating and cooling is shown versus temperature in Figure 5. The total expansion at 1100 °C for the sample was 0.55 %. Thermal expansion coefficient from 20 to 1100 °C is estimated to $5.14 \cdot 10^{-6}$ /K.

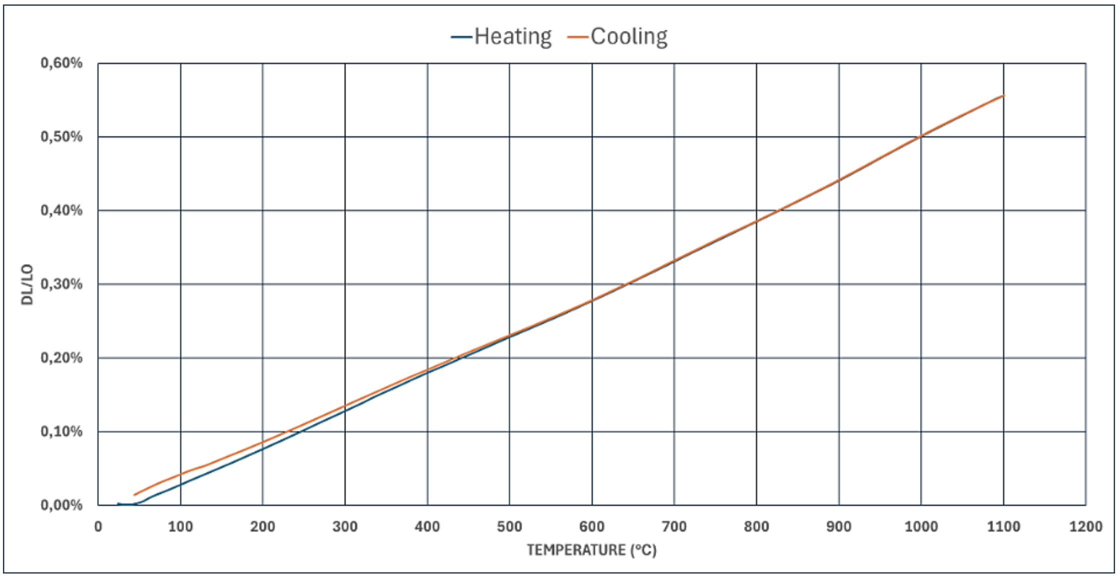

Figure 5. Thermal expansion from room temperature (20 °C) to 1100 °C.

4.3 Thermal Conductivity

The thermal conductivity of two samples (inner and outer) was determined from room temperature up to 1000 °C by the laserflash method using a NETZSCH LFA 457 Microflash instrument (NETZSCH-Gerätebau GmbH, Germany). The thermal diffusivity (*a*) and the specific heat (*Cp*) were determined using the measured signal. To calculate the thermal conductivity, the density and the specific heat capacity were needed for all temperatures.

The thermal conductivity (λ) was determined using the thermal diffusivity, the specific heat capacity and the density (ρ):

$$\lambda(T) = a(T) \cdot Cp(T) \cdot \rho(T) \quad (1)$$

The density at elevated temperatures was determined by the density measured at room temperature and the thermal expansion of the material. The sample size was 25.4 mm (1 inch) in diameter and 2 mm in thickness.

The thermal conductivity measurements for the two samples inner and outer are shown in Figure 6.

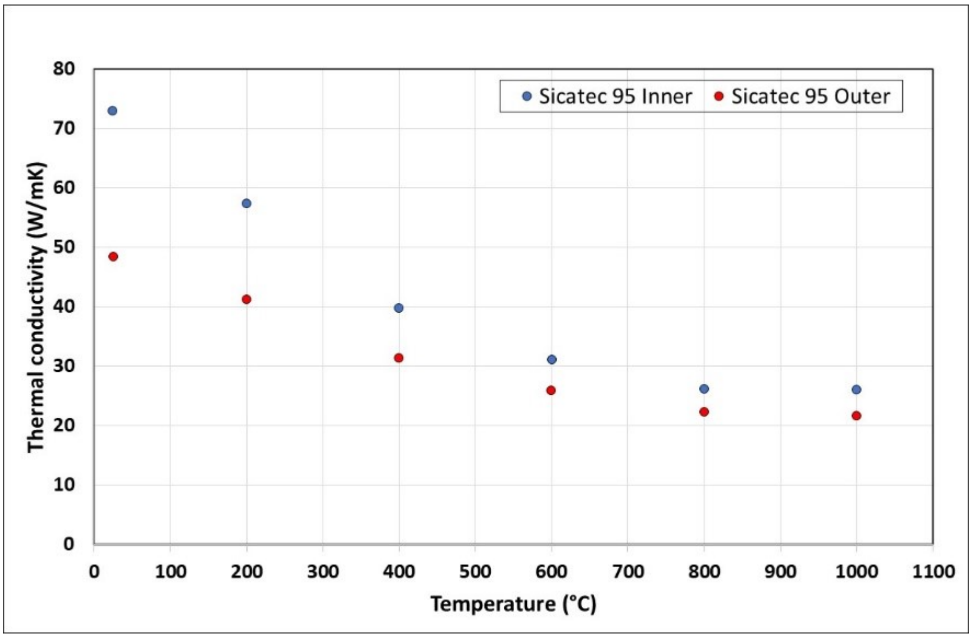

Figure 6. Thermal conductivity from room temperature (20 °C) to 1000 °C for inner and outer sample.

4.4 Oxidation Resistance

The oxidation test was performed by suspending the sample (60 × 30 × 15 mm) in a balance in a resistance heated tube furnace. The furnace was heated to 950 °C at a rate of 300 °C/h and then kept at 950 °C for 100 hours. A constant flow of 50 mL/s of synthetic air was maintained through the furnace throughout the entire test duration. The course of oxidation in terms of weight change of the sample was recorded continuously during the test.

The weight of the sample before and after the oxidation test are shown in Table 4. The recorded weight change of the samples versus time is illustrated in Figure 7 for the samples marked inner and outer.

Table 4. Weight of samples inner and outer before and after oxidation.

Outer sample			Inner sample		
Before (g)	**After (g)**	**Weight increase (%)**	**Before (g)**	**After (g)**	**Weight increase (%)**
66.67	67.53	1.29	67.00	67.81	1.21

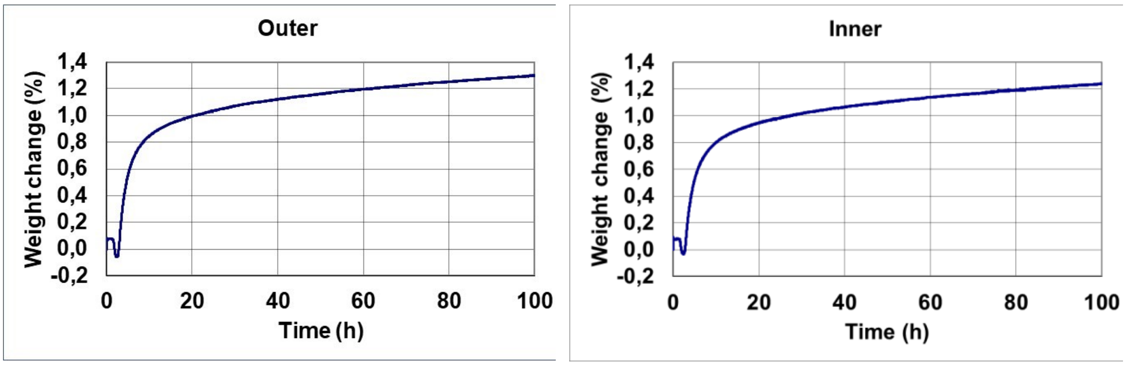

Figure 7. Weight changes as a function of time for outer and inner samples.

We also registered the weight changes during the heat-up period, and we observed some weight loss starting at 550 °C. This is possible due to some carbon burning off in the air. The registrations are shown in Figure 8 for both outer and inner sample.

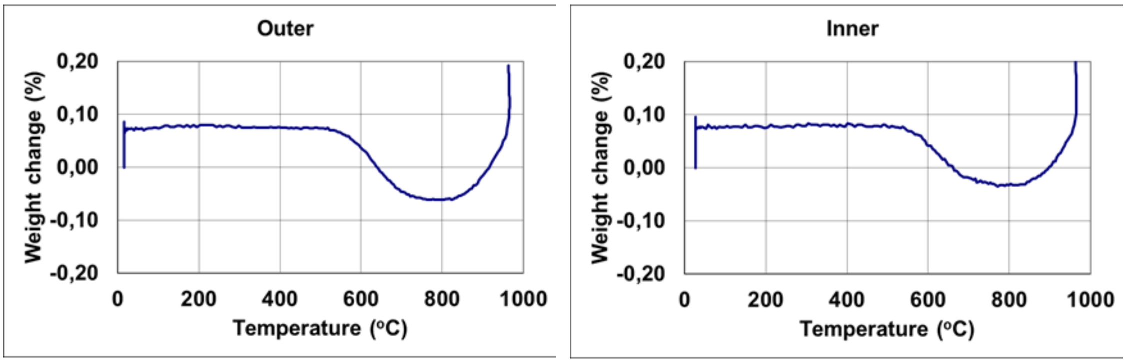

Figure 8. Weight change during heat-up for outer and inner samples.

4.5 Chemical resistance SINTEF and LIRR method

Chemical resistance was measured by using the SINTEF test cell developed in the mid-90's. The test method and relating results have been described in many publications [1–6]. The aim of the test is to simulate the chemical conditions of industrial cells, namely: aluminium metal, fluoride electrolytes, fluoride vapours (HF, $NaAlF_4$) and gas from the anode (mainly CO_2 and CO). The test is running for 50 h.

The test cell, shown in Figure 9, consists of a graphite crucible lined with sintered alumina tube (Alsint, Haldenwanger) and covered with a lid of graphite. A plate of TiB_2-graphite composite (TiB_2 - G, Great Lakes) covered the bottom of the crucible to ensure a stable level of aluminium in the crucible (Al wets TiB_2-graphite well), and it also acted as a current collector. A graphite anode (diameter = 1.5 cm) was placed in the middle of the cell and immersed about 2–2.5 cm into the electrolyte. The four test pieces were placed symmetrically around the anode. The test cell was kept in a closed vertical tube furnace under argon atmosphere (outside the crucible). The temperature was measured with a thermocouple (Pt10Rh) placed in the crucible wall. Before the electrolysis started, the temperature was also checked with a thermocouple placed in the middle of the electrolyte. The electrolyte composition is 10 wt % AlF_3, 5 wt % CaF_2, 7 wt % Al_2O_3 and remaining Na_3AlF_6. The temperature during the test was 955 °C. The anode current was 2 A. Temperature, current and cell voltage were monitored during the test.

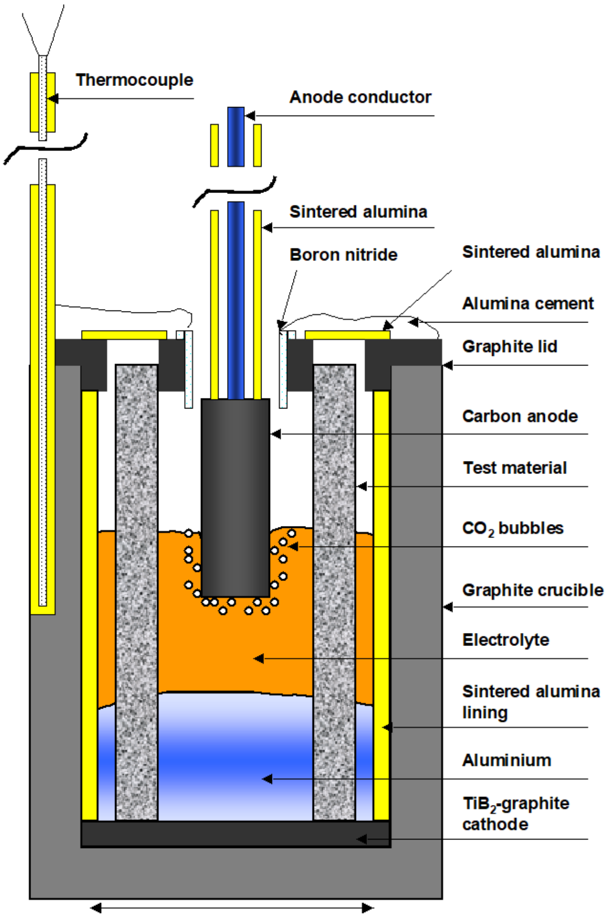

Figure 9. Chemical resistance SINTEF test cell.

After electrolysis, the crucible with the test pieces was cooled down. The graphite lid was then removed, and the rest of the test cell was again heated up in an open furnace, and the test pieces were taken out of the crucible when the bath was melted.

The degree of degradation is determined by the volume loss of the pieces during the test. The volume loss of each piece was determined (volume before - volume after) and related to the degree of degradation as shown in Table 5. Volume loss [%] = [(volume before – volume after) / volume before] x 100 %.

Table 5. Evaluation of the degree of degradation based on volume loss.

Volume loss (%)	Degree of degradation
< 0,1	0
0.11 – 1.00	1
1.01 – 2.00	2
2.01 – 3.00	3
3.01 – 4.00	4
4.01 – 5.00	5
5.01 – 6.00	6
6.01 – 7.00	7
7.01 – 8.00	8
8.01 – 9.00	9
> 9.00	10

This test was successfully run with self-bonded SiC samples. The cell voltage and temperature during the test are shown in Figure 10. The anode was changed after 25 h. The anode consumption was measured to be 11.19 g in total for the 2 anodes used.

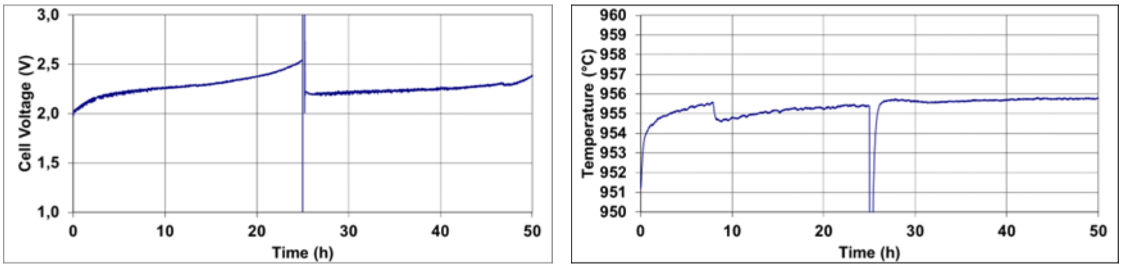

a) Cell voltage b) Temperature

Figure 10. Cell voltage and temperature during the 50-h test period. a) cell voltage and b) temperature.

The test samples after the test are shown in Figure 11. As can been seen, the degradation was minimal. We can see some attacks in the gas phase zone but in total we measured near zero degradation leading to 0 rating on the 0-10 scale presented in Table 5. The samples were infiltrated by electrolyte/metal, as a result we measured a weight increase around 10–11 % and a porosity decreased to around 3 % open porosity. The samples were densified but not degraded.

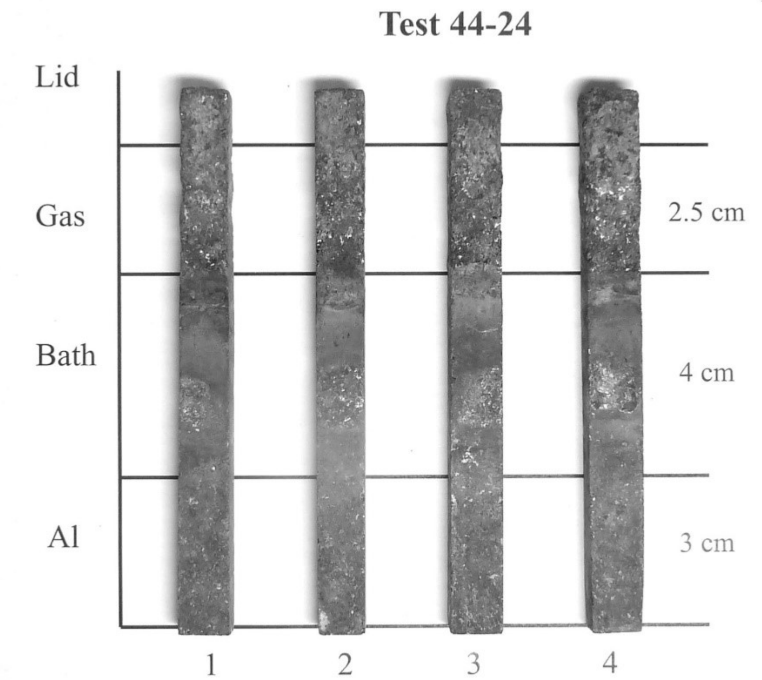

Figure 11. Test samples after the SINTEF test.

LIRR have also developed a chemical resistance test method [7]. The test simulates the actual working conditions in reduction cells when no side-ledge is present. After the test, the specimens' volume loss is measured to evaluate their cryolite resistance capacity. Four T-shaped specimens with dimensions 20/30 × 20 × 120 mm are prepared for the test (Figure 12). The test device (Figure 13) can accommodate 4 specimens at a time.

The test is running for 24 h in a cryolitic bath with 88 wt % Na_3AlF_6, 5 wt % CaF_2 and 7 wt % Al_2O_3 at a temperature set to 1000 °C. The samples rotate at a speed equal to 45 rpm. CO_2-gas is purged into the electrolyte with a flow rate around 1 L/min.

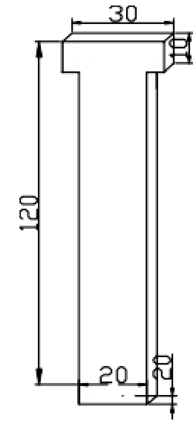

Figure 12. T-shaped specimen.

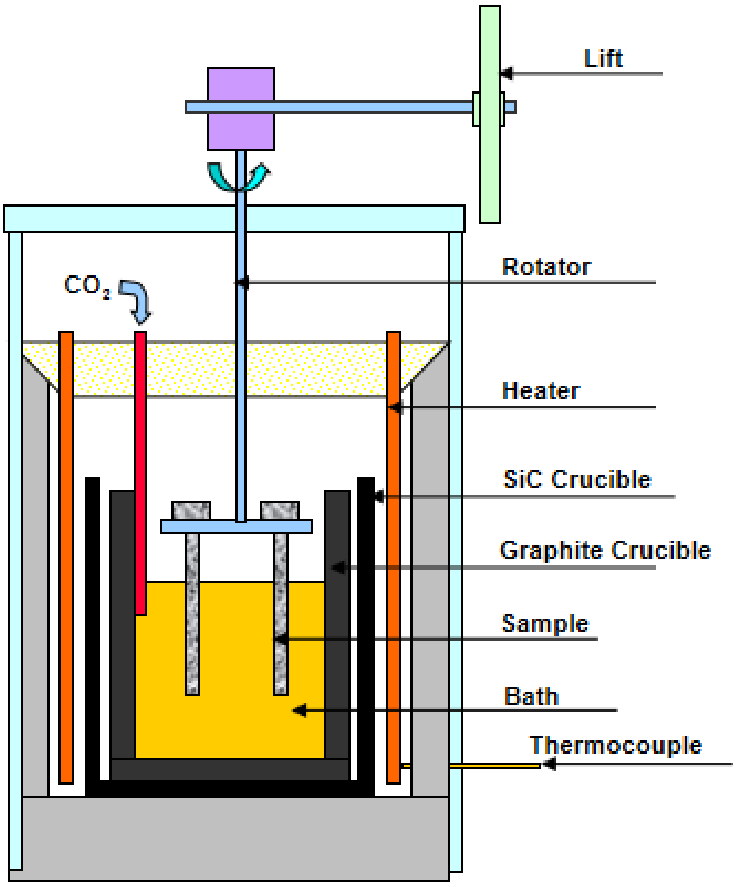

Figure 13. LIRR's test cell.

The degree of degradation is determined by the volume loss of the specimens. The volume is measured in accordance with ISO 5017.

A scale from 0–6 shown in Table 6 is used to assess the degree of degradation.

Table 6. Scale for degree of degradation.

Volume loss (%)	Degree of degradation	Evaluation
0.00 - 4.00	1	Perfect
4.01- 8.00	2	Excellent
8.01- 12.00	3	Very good
12.01 - 16.00	4	Good
16.01 - 20.00	5	Accepted
> 20.00	6	Rejected

LIRR tested 4 samples in the test set-up and the samples after the test are shown in Figure 14. The degree of degradation was 1.

Figure 14. Tested samples after the LIRR test.

5. Conclusions

The test and analysis performed on self-bonded SiC samples shown the following results:

- Homogenous structure – small differences within the block thicknesses.
- SiC content: 93–94 wt %, Si_2ON_2: 6–7 wt % and Si: 0.1 wt %.
- Relative low porosity and high density.
- Oxidise in air with 1.2 wt % increase after 100 h at 950 °C.
- Thermal expansion around 0.55 % at 1100 °C.
- Relatively high thermal conductivity.
- Very good chemical resistance.

Based on laboratory test results it seems that the self-bonded SiC materials have a more homogeneous microstructure, lower porosity, higher density and show better chemical resistance and higher thermal conductivity than traditionally Si_3N_4-SiC materials.

Further development and tests should be conducted in industrial cells. Valuable experiences will then be obtained with autopsies and further analysis and experiences.

6. References

1. Egil Skybakmoen et al., Quality evaluation of nitride bonded silicon carbide sidelining materials, *Light Metals* 2005, 773–778 https://doi.org/10.1002/9781118647745.ch114
2. Egil Skybakmoen et al., Test and analysis of nitride bonded SiC sidelining materials. Typical properties analysed 1997–2007," *Light Metals* 2008, 943–948.
3. Egil Skybakmoen, Zhaohui Wang and Tor Grande, The influence of microstructure of Si_3N_4-SiC side-lining materials on chemical/oxidation resistance behaviour tested in laboratory scale, *Proceedings of the 11th Australasian Aluminium Smelting Technology Conference*, Dubai, UAE, 6–11 December 2014, Paper 22W3.
4. Egil Skybakmoen and Zhaohui Wang, Experience from laboratory testing of commercial silicon bonded silicon carbide materials, Typical properties and analyses, *Proceedings of 35rd International ICSOBA Conference*, Hamburg, Germany 2–5 October 2017, Paper AL20, *TRAVAUX* 46*,* 973–986.
5. Egil Skybakmoen, Laboratory evaluations of ceramic sidelining materials, *Proceedings of the 37th International ICSOBA Conference and XXV Conference «Aluminium of Siberia»*, Krasnoyarsk, Russia, 16–20 September, 2019, *TRAVAUX* 48*,* 1035–1045.
6. Egil Skybakmoen, Quality Evaluation of Nitride–Bonded SiC Sidelining Materials: Historical Trends 1997–2022 Including Results and Development of Test Methods, *Light Metals* 2022, 921–928 https://doi.org/10.1007/978-3-030-92529-1_120
7. Junguo Zhao et al., Test method for resistance of SiC material to cryolite, *Light Metals* 2006, 663–666.